Journal of Materials Chemistry A

Accepted Manuscript

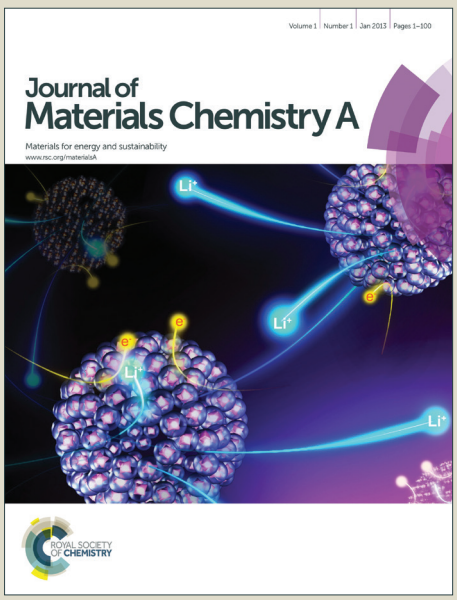

ROYAL SOCIETY OF CHEMISTRY

www.rsc.org/materialsA

Cite this: DOI: 10.1039/c0xx00000x

www.rsc.org/xxxxxx

ARTICLE TYPE

In situ Preparation of Novel Organo-Inorganic (6, 13-Pentacenequinone: TiO_2) coupled Semiconductor Nanosystem: A new Visible Light active Photocatalyst for Hydrogen Generation

Vikram Pandit,[a] Sudhir Arbuj, [a] Ranjit Hawaldar, [a] Pradnya Kshirsagar,[a] Uttam Mulik, [a] Suresh Gosavi,[b] Chan-Jin Park*,[c] Bharat Kale*, [a]

Received (in XXX, XXX) XthXXXXXXXXX 20XX, Accepted Xth XXXXXXXXX 20XX
DOI: 10.1039/b000000x

Studies related to synthesis of stable UV-Visible light active photocatalyst for hydrogen generation has been limited to only inorganic semiconductors, their nanostructures and hetero-structures. Hence, in the present investigation, organo-inorganic (6, 13- Pentacenequinone (PQ): TiO_2) coupled semiconductor nanosystem has been demonstrated as an efficient visible light active photocatalyst for hydrogen production for the first time. The 3-5 nm anatase TiO_2 nanoparticles have been uniformly decorated on thin sheets of monoclinic PQ by in-situ solvothermal method. These as prepared PQ: TiO_2 coupled semiconductor nanosystems exhibited band gap in the range of 2.7-2.8 eV. The strong emission observed at 590 nm can be attributed to transfer of electrons from the LUMO energy level of TiO_2 combine with the holes present at HOMO level of PQ. Furthermore, this electron-hole recombination makes availability of electrons and holes in LUMO of PQ and HOMO of TiO_2, respectively. Hence, this hybrid semiconductor coupled nanosystem conferred utmost hydrogen evolution i.e. 36,456 µmol/h/g from H_2S under UV-visible light which is four times higher than TiO_2 as well as earlier report of UV-visible light active photocatalyst. The enhanced activity is obtained for the PQ: TiO_2nanosystem has been discussed, thoroughly. Our results open up a new path to explore various inorganic systems coupled with PQ as a new photoactive hybrid catalyst for various chemical and physicochemical processes.

Introduction

Nanomaterial's have aroused considerable interest due to their fascinating size-dependent optoelectronic, magnetic, chemical, and other physical properties.[1-3] Now, it is renowned that for the fabrication of next-generation optoelectronic devices and for fulfilling the energy demand, the use of nanoscale semiconductor nanostructures are absolutely essential.[4-6] In this context, great efforts have been dedicated by researchers for the synthesis of multi-functional nanomaterial's. Nanostructured semiconductor materials are known to act as efficient photocatalyst due to their high surface and different morphologies.[7,8] Numerous strategies have been employed to achieve efficient photocatalysts by using surface-tuning strategies for synthesis of various oxides at nanoscale.[9] In the past decade, though there has been noteworthy progress in the field of photocatalysis[10] but most of it has been limited due to use of ultraviolet (UV) light instead of most useful visible–light region. Consequently, scientific and engineering interests in semiconductor photocatalysis have grown significantly in researchers.[10] The researchers have explored visible light (renewable source) active photocatalyst for hydrogen production, which is essential for economical hydrogen production.[10, 11] Hydrogen has been recognized as a future fuel and capable to meet the global energy demand. Using the photocatalysis process, the H_2 can be produced from H_2O as well as H_2S, economically. Since, H_2S is abundantly available as a waste gas from oil refineries and alkali chemical industries, presently, the ubiquitous Claus process is used for H_2S utilization to produce sulphur instead of hydrogen. Hence, photocatalytic hydrogen production from H_2S has immense importance. Considering the importance of hydrogen as a future fuel, hydrogen production by photocatalytic process using UV-Visible light has immense importance. Photocatalytic hydrogen production from hydrogen sulphide and water are economically more viable as compared to conventional hydrogen production methods such as steam reforming, electrolysis etc.[8-12] Hence, we have utilized the abundant waste H_2S to produce eco-friendly hydrogen under UV-Visible light.[8,13-16] Few reports are available

on visible light active photocatalyst for hydrogen production from H_2S. The main efforts were taken to develop the visible light active photocatalyst. In this context, metal oxide semiconductors have been doped with transition metal as well as anions for narrowing the band gap suitable for UV-Visible light.[17-23] Considering the TiO_2 as one of the best stable, eco-friendly and economical photocatalyst, massive work has been performed on doping of TiO_2 with cations and anions for narrowing the bandgap.[6,9] Recently, TiO_2 graphene nanocomposites and decoration of Ag, Au, and Pt on TiO_2 have also been reported as a visible light active photocatalyst.[11, 24-34]

In this article, considering the good stability of TiO_2 and our earlier report of 6, 13- Pentacenequinone (PQ) organic semiconductor as a best photocatalyst for energy harvesting and environmental remediation, we have investigated efficient organo-inorganic hybrid (PQ: TiO_2) nanosystem as a visible light active photocatalyst for hydrogen production for the first time.[16] The PQ has good thermal stability and band gap around 2.8 eV. It has also simple synthesis procedure along with higher molar absorption coefficient. This makes PQ as an efficient visible light active photocatalyst. The in-situ preparation of novel organo-inorganic (PQ: TiO_2) coupled semiconductor nanosystem has been investigated using facile solvothermal method. The interesting optical properties of this organio–inorganic coupled nanosystem have been discussed and justified the enhanced photocatalytic activity.

During the solvothermal preparation of TiO_2, PQ has been introduced which confer PQ: TiO_2 hybrid nanosystem. The PQ: TiO_2 nanosystems are prepared using 5, 10 and 17 mmol of titanium tetra-isopropoxide precursor and termed as PT-5, PT-10 and PT-17, respectively, throughout the manuscript. This unique nanosystem has been characterized further for phase identification.

Results and Discussion

These as prepared PQ: TiO_2 nanosystems were characterized by X-ray diffractometry (XRD) and depicted in Figure 1. XRD patterns pertaining to pure PQ and TiO_2 are also shown in Figure 1a, e).

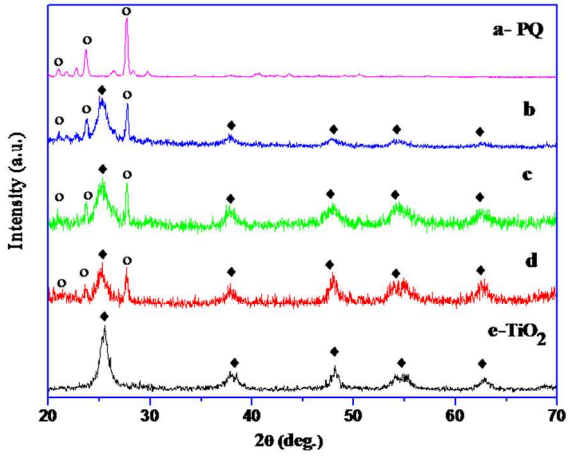

Figure 1.XRD patterns of PQ: TiO_2 hybrid nanosystem where a) PQ, b) PT-5, c) PT-10, d) PT-17 and e) TiO_2

In the XRD patterns of nanosystems (Figure 1b-d), the diffraction peaks at 2θ = 25.3, 37.8, 48, 53.9 and 55° can be indexed as (101), (004), (200), (105) and (211) corresponds to anatase TiO_2 (JCPDS No. 21-1272). The diffraction peaks at 2θ =14.7, 23.6 and 27.7° represent (012), (112) and (104) planes which indicates the existence of crystalline monoclinic phase of PQ (JCPDS No.47-2123).The broadening of the XRD peaks of TiO_2 clearly shows nanocrystalline nature of the material. The crystallite size of TiO_2 calculated in PT-5, PT-10 and PT-17 hybrid nanosystem using Scherrer's formula and was observed to be 5.8, 6.6 and 7.5 nm, respectively. However, with increase in TiO_2 concentration, the overall intensity of the other TiO_2 peaks also increased slightly with retaining the broadness. The difference is quite marginal and difficult to compare visibly because the crystallite size difference is not much (~ 1 nm). However, it has been also studied using SAED pattern and discussed in morphological study. The existence of monoclinic PQ and anatase TiO_2 in the XRD clearly indicates the formation of organo-inorganic (PQ: TiO_2) hybrid nanosystem.

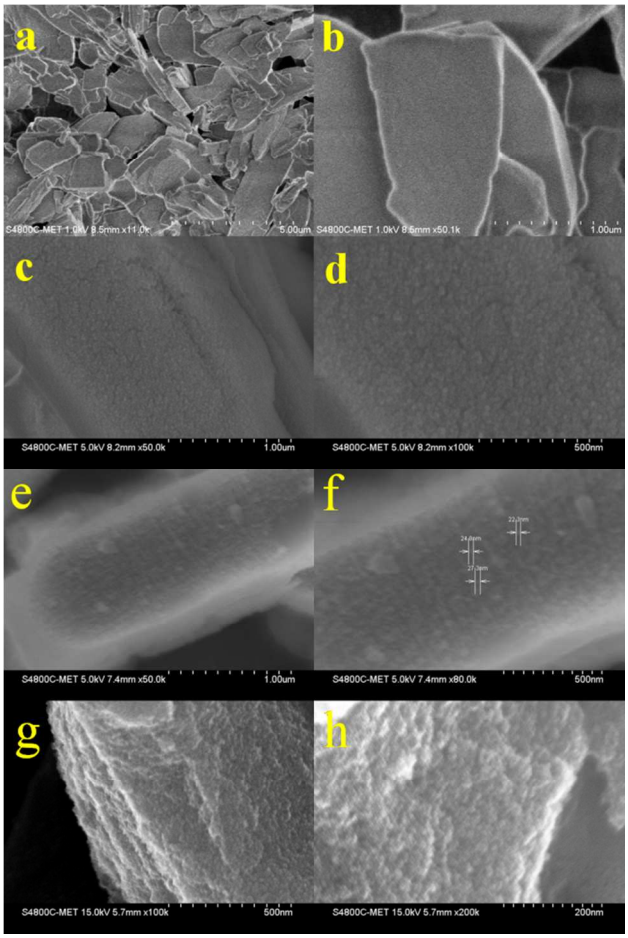

Figure 2.FESEM of PQ: TiO_2 hybrid nanosystem (a, b) PQ, (c, d) PT-5, (e, f) PT-10, and (g, h) PT-17

FESEM images of as prepared PQ: TiO_2 hybrid nanosystems i.e. PT-5, PT-10 and PT-17 are shown in Figure 2. The pristine PQ observed in the form of micron-sized sheets with smooth surface having thickness in the range of 50 to 200 nm (Figure 2a, b). FESEM images of PT-5 nanosystem indicate the formation of nanosized TiO_2 particles having size ≤ 5 nm on the surface of PQ sheets (Figure 2c, d). Whereas, PT-10 and PT-17 hybrid

nanosystems showed 5-7 and 8-10nm sized TiO_2 particles uniformly layered on PQ sheets (Figure 2e-h). All the three prepared hybrid nanosystems depict the same morphology having nanosized TiO_2 particles on the surface of PQ sheets. More FESEM images with high resolution are given in supporting information (Fig. S1). It is also observed that the density of the nanoparticles increases from PT-5 to PT-17 which is quite obvious because of the increase in the TiO_2 concentration. Moreover, the TiO_2 nanoparticle clusters were also seen sandwiched between the PQ sheets. Overall, FESEM images clearly show the uniform distribution of the TiO_2 nanoparticles on the PQ sheet for all the prepared nanosystems.

The TEM images with SAED pattern of prepared PQ: TiO_2 hybrid nanosystems are depicted in Figure 3. The hybrid PT-5 nanosystem (Figure 3a, b) confirms the formation of spherical shaped TiO_2 nanoparticles having size in the range of 3-5 nm (inset of Figure 3b). Also, TEM images of PT-10 and PT-17 hybrid nanosystems validates the existence of TiO_2 nanoparticles having sizes 6-8 and 9-10 nm, which are evenly distributed on PQ sheets (Figure 3c-f). High resolution TEM images are depicted in supporting information indicating size and shape of TiO_2 particles (Fig. S2).

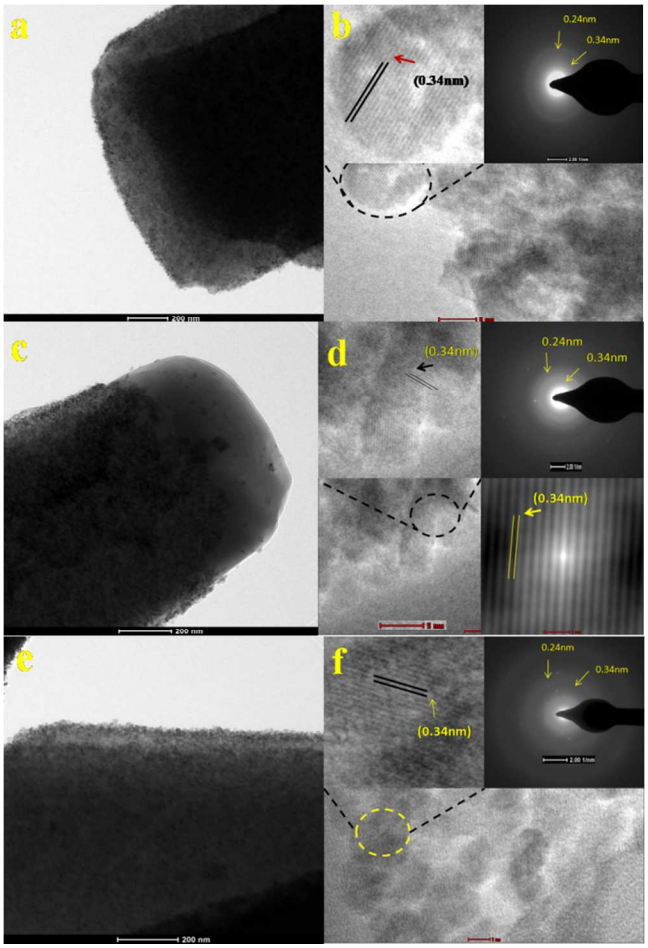

Figure 3.TEM images of PQ: TiO_2 nanosystem (a, b) PT-5, (c, d) PT-10, and (e, f) PT-17, inset of Figure 3(b, d, and f) indicates the HRTEM and SAED pattern of PQ: TiO_2.

The well-defined lattice fringes are seen in the HRTEM images (as a inset of Figure 3b, d& f) and the inter-planer distance between the adjacent planes was observed to be 0.34nm which corresponds to 101 plane of anatase TiO_2, thereby confirming the formation of anatase phase of TiO_2 in all the three hybrid PQ: TiO_2 nanosystems. The SAED pattern (inset of Figure 3b, d, and f) also shows d spacing of 0.24 and 0.34 nm attributed to (103) and (101) reflection planes matching with anatase TiO_2 in all three nanosystems, respectively. The ED pattern clearly shows that the intensity of bright rings increases from PT-5 to PT-17 indicates slight increase in crystallinity which was very imprecise to see from XRD. The HRTEM clearly depicts the perfect interface between TiO_2 nanoparticles and PQ nanosheets. This interface could provide the proper channel for electrons and holes transfer between PQ and TiO_2 semiconductors. The detail study about the electron transfer is given in optical study section.

The diffuse reflectance UV-Visible absorbance spectra of PQ loaded TiO_2 are depicted in Figure 4. Pristine PQ shows absorbance edge at 449 nm indicating band gap around 2.8 eV.

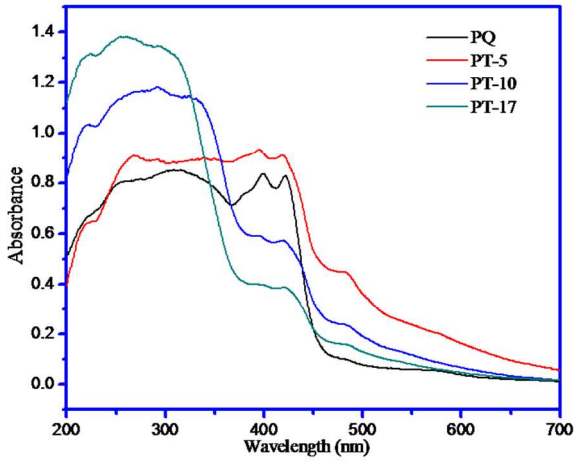

Figure 4. Diffuse reflectance UV-Visible absorbance spectra of PQ: TiO_2 hybrid nanostructures a) PQ, b) PT-5, c) PT-10 and d) PT-17

The nanosystem PT-5 shows absorption edge at 451nm having band gap of 2.74 eV, however, PT-10 and PT-17 nanosystem shows two distinct absorption edges at 380 nm (band gap 3.26 eV),and 455 nm (band gap 2.73 eV), corresponds to TiO_2 and PQ, respectively. The higher band gap of TiO_2 in PT-10 and PT-17 are due to blue shift in the absorbance as a function of particle size. The band gap values are verified using Tauc's plot (Supporting information Fig. S3). This confirms the formation of coupled hybrid nanosystem of PQ: TiO_2 (Figure 4c, d).

The increase in absorbance in the range of 370 to 400 nm attributed to increased concentration of TiO_2 in prepared nanosystem. In case of sample PT-5, we observed clear single absorption peak due to higher concentration of PQ. Overall, the absorbance peak in the range of 400 to 460 nm corresponds to PQ and 370 to 400 nm corresponds to TiO_2 in PT-10 and PT-17 hybrid nanosystem.

The photoluminescence spectra are often employed to study surface processes involving the electron-hole fate of the semiconductors. Figure 5 represents the photoluminescence spectra of hybrid nanosystems PT-5, PT-10, PT-17 along with pure PQ and TiO_2, respectively. The prepared nanosystem show strong emission peaks at 550 nm with satellite peak at 590 nm. Increase in PL intensity as a function of TiO_2 concentration is observed.[35-38]

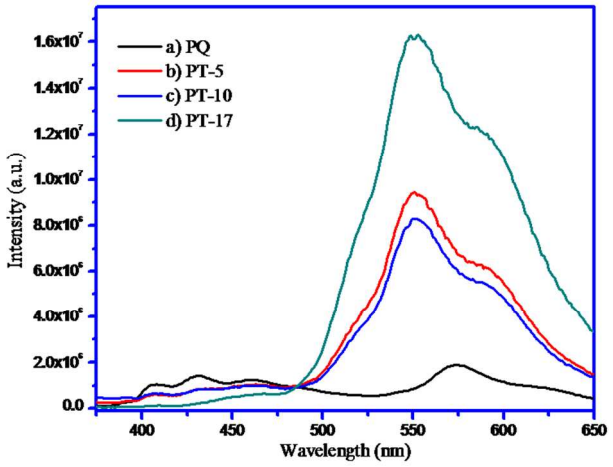

Figure 5. Photoluminescence spectra of PQ: TiO_2 hybrid nanosystem a) PQ, b) PT-5, c) PT-10 and d) PT-17

The peak at 550nm might be due to the certain defects generated because of oxygen vacancies. Such defects acts as self trap centres for the excitons recombination owing to combine effect of defects canters generated from oxygen vacancies and lower particle size. PT-5 is showing slightly higher PL emission at 550 nm compared to PT-10, this might be because of the lower particles size of TiO_2 which leads the self-trapped exciton recombination as discussed earlier. *Lin et al* reported that the emission peaks at 550nm is attributed to electronic transitions involving traps states.[40] A report by *Zhang et.al*. on the photoluminescence study of anatase TiO_2 nanoparticle is in good agreement with our results.[32] The satellite peak at 590 nm might be due to electron-hole recombination.

For simplicity, we studied the HOMO and LUMO energy levels of PQ and TiO_2. Figure 6 shows the band diagram of coupled nanosystems.

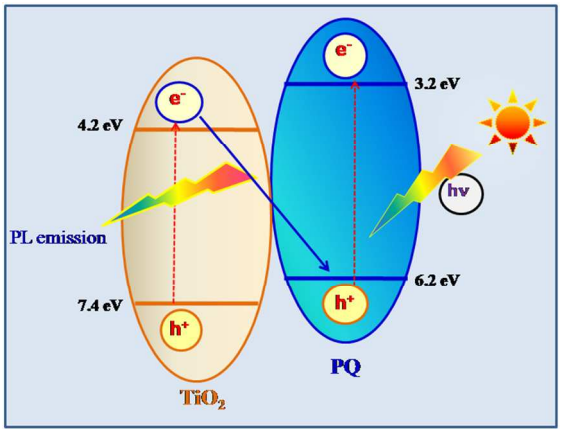

Figure 6. Schematic band structures of PQ: TiO_2 hybrid nanosystem

The LUMO energy levels of PQ and TiO_2 have values of 3.29 and 4.20 eV, whereas the HOMO level values are 6. 29 and 7.40 eV, respectively.[16, 39] Upon excitation with 350 nm light, the electron-hole pairs were generated in both the semiconductors, PQ and TiO_2. Due to coupling of these two semiconductors, the electron from LUMO energy level of PQ transfer to the LUMO of TiO_2 which may later on combine with the hole present in the HOMO level of PQ. This electron-hole recombination might be responsible for the emission peak at 590 nm confirmed by PL study (Fig.5).

In the present nanosystem, spherical nanoparticles of TiO_2 with 3-5 nm (PT-5) size are intact on plate like structure of PQ (organic semiconductor); hence, the generated electron-hole pairs can be easily moved across the organic-inorganic interface.

Reports are also available mentioning that the emission peak at 550 nm may be due to mid trap states.[34] The pristine PQ indicates the emission peaks at 408, 432 and 574 nm, the peak at lower wavelength are due to π to π* and n to π* whereas the emission peak at 574 nm might be due to certain mid trap centers. The enhance PL intensity in the prepared hybrid system is result of proper electron transfer between organic-inorganic semiconductor which could inhibits the non-radiative electron-hole pair recombination's. The observed results are in agreement with the reported one wherein for the hetero-systems of TiO_2, with particle size less than 10 nm shows intense yellow-green emissions. [37-39]

Photocatalytic study

Photocatalytic study was performed using synthesized PQ: TiO_2 hybrid nanosystems i.e. PT-5, PT-10 and PT-17 under UV-Visible light for hydrogen generation using H_2S.

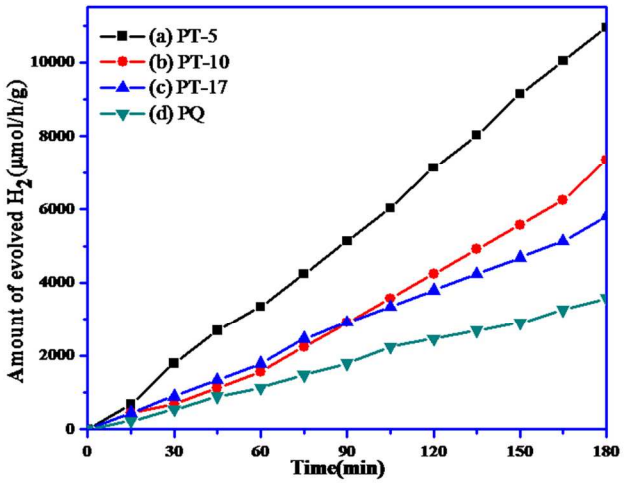

Figure 7. Photocatalytic activity of PQ: TiO_2 hybrid nanosystems (250 mL reactor, 0.1 g catalyst, feeding rate of H_2S gas 0.5 mL/min.)

Figure 7 represents the time dependent photodecomposition of H_2S which clearly shows stable linear increase in the hydrogen evolution. The utmost hydrogen evolution rate i.e. 36,456 μmol/h/g was obtained for PT-5 hybrid nanosystem (Table1) and slightly lower for PT-10 and PT-17.The present hydrogen evolution rateobtained is four times higher than TiO_2 as well as also superior than earlier reports.[13-16, 24]

Table 1: Photocatalytic Hydrogen evolution

Sr. No.	Name of the catalyst	H_2 evolution (μmol/h/g)
1	PT-17	18600
2	PT-10	24552
3	PT-5	36456

The hydrogen evolution obtained is much higher than earlier reports as well as P-25 DegussaTiO_2 and PQ for the feeding rate of H_2S at 0.5 ml/min. At this minimum H_2S flow rate, continuous hydrogen production has been monitored. As the

initial rate of H_2S feeding is higher, the hydrogen evolution rate is also increases, accordingly and hence 0.5 ml/min feeding rate is maintained throughout the experiment.[16] It is noteworthy that excellent hydrogen evolution rates observed at this feeding rate. In 0.25 M KOH solution (pH 12.5), the weak diprotic acid H_2S (pKa values are 7.0 and 11.96) dissociates and maintains equilibrium with hydrosulfide HS^- ions (1). The PQ: TiO_2 hybrid nanosystem absorbs light and generates electron-hole pairs (2). The photogenerated valence band hole (h^+VB) upon band gap excitation of PQ: TiO_2 hybrid nanosystem oxidizes the HS^- ion to disulfide ion (S_2^{2-}), liberating a proton from the HS^- ion (3). The conduction band electron (e^-CB) from PQ:TiO_2 hybrid nanosystem photocatalyst reduces protons to produce molecular hydrogen (4).

$$H_2S+OH^- \longleftrightarrow HS^-+H_2O \quad (1)$$

$$\text{Semiconductor PQ:}TiO_2 \longleftrightarrow h^+VB + e^-CB \quad (2)$$

$$\text{Oxidation: } 2HS^- + 2h^+VB \longleftrightarrow S_2^{2-}+2H^+ \quad (3)$$

$$\text{Reduction: } 2H^+ + 2e^-CB \longleftrightarrow H_2 \quad (4)$$

We did not observe any hydrogen evolution without catalyst and in dark; this clearly indicates the hydrogen evolution is due to PQ: TiO_2hybridnanosystems.

The mechanistic approach for photocatalytic H_2 generation via H_2S decomposition over prepared PQ: TiO_2hybrid nanostructures are depicted in Figure 8. The PT-5 exhibits higher photocatalytic activity as compared to other prepared nanosystems. The conduction band (CB) of TiO_2 is 0.91 eV lower than the CB of PQ and valence band (VB) of TiO_2 is ~1.11 eV lower than VB of PQ, respectively. Upon excitation with light, there are two possibilities: (1) the electron-hole pairs generated in both the semiconductors and generated species acts as a reducing as well as oxidizing agents to generate H_2 and (2) the CB electrons of TiO_2 recombine with VB hole of PQ. The H_2 generation takes place at CB of PQ and oxidation reaction occurred at VB of TiO_2.

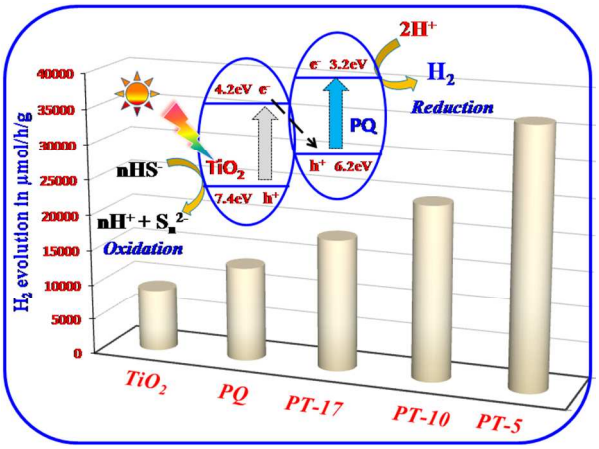

Figure 8.Mechanism of H_2 generation

This process results in the availability of electron for H_2 generation by inhibiting the electron-hole recombination in the individual semiconductor. The PL study supports the reaction mechanism and reveals that activity of nanosystem found to be decreased with increase in PL emission. The PL study clearly support that the emission peak around 550 nm confer the recombination of electron-hole pairs where large number of electrons transfer from CB of PQ to CB of TiO_2 and recombine with holes present in VB of PQ or TiO_2. The PT- 17 nanosystem is having higher PL intensity and hence shows lower H_2 generation. Additionally, the reduction in the nanoparticles size of TiO_2 intact on PQ in the sample PT-5 and PT-10 also affects the H_2 generation. The reduction in PL intensity in these samples may be due to lower size of TiO_2 which creates defects. These defects are responsible for suppression of charge carrier recombination which ultimately enhances the photocatalyticactivity.[15] However, though PT-5 has slightly higher intensity than PT-10 but combine effect with lower particle size enhance the inhibition in the charge carrier recombination (as discussed in PL study) which ultimately confer utmost activity.[40] Another noteworthy advantage of coupled semiconductor systems is that it allows inter-particle electron transfer which enhances charge separation and help for enhancement in photocatalytic activity. Considering the very small nanoparticles of TiO_2 (3-5 nm) in intimate contact with PQ, the surface trapping of electrons and holes before recombination will also be more efficient.[40] The photo generated electron hole pairs have a much shorter distance to travel to reach the surface in a small cluster. Once, the charged carriers (electron and holes) trapped at the interface, and then they can participate in redox reactions and contribute in enhancement of photocatalytic activity.

Conclusions

In nutshell, the novel organo-inorganic PQ: TiO_2 hybrid semiconductor nanosystems have been successfully synthesized by facile solvothermal method. The nanosystems have been used as a photocatalyst for the photodecomposition of H_2S to produce hydrogen under UV-visible light. The utmost hydrogen evolution i.e. 36,456 µmol/h/g has been observed over a naked (without co catalyst) PQ: TiO_2 hybrid nanosystem under UV-Visible light. In this hybrid nanosystem, very small nanoparticles of TiO_2 are intact with sheets of PQ which exhibit most efficient inhibition of charge carrier recombination which is responsible for enhanced photocatalytic activity. The prima-fascia result shows that organo-inorganic hybrid nanosystem providing a promising choice of efficient UV-Visible light active photocatalyst. It is noteworthy that other hybrid nanosystems with other semiconductor oxide can be synthesized with the present technique.

Experimental

Catalyst Preparation

For the synthesis of PQ: TiO_2 nanosystem, 5 ml of titanium tetra-isopropoxide (17 mmol) in methanol, 2 ml of hydrazine hydrate was stirred in beaker. To this solution 3.05 g (17 mmol) of guanidine carbonate solution in acetic acid was added. The solution was further stirred for 15 min and appropriate amount (0.25 g) of freshly prepared PQ was added and continued the stirring for 15 min. PQ was prepared as per the previously reported method. The resultant reaction mixture was transferred to a Teflon-lined autoclave; furthermore, this Teflon lined reactor was sealed and heated at 150ºC for 15 h in oven. The obtained precipitate of PQ: TiO_2 was washed and dried at 80°C. Similar procedure was followed using different concentrations of titanium tetra-isopropoxide i.e. 10 and 5 mmol. The PQ:

TiO_2nanosystem prepared using 5, 10 and 17 mmol of titanium tetra-isopropoxide precursor were termed as PT-5, PT-10 and PT-17, respectively.

Catalyst Characterization

Structural studies of the as-synthesized products were performed using an X-ray diffractometer (XRD-D8, Advance, Bruker-AXS). Morphological study of the samples was performed using Field Emission Scanning Electron Microscopy (FESEM, Hitachi S-4800) and a Transmission Electron Microscope (TEM, Philips, EM-CM-12). UV-Visible absorbance spectra were recorded using Shimadzu UV-vis-NIR spectrophotometer (Model UV-3600) over a wavelength range of 200 to 800 nm.

Photocatalytic Study

The hydrogen evolution was performed in a quartz photo-reactor using 0.1 g of PQ: TiO_2 under the irradiation of 450W Xe lamp light source (Oriel). The cylindrical quartz reactor was filled with 250 mL, 0.25 M aqueous KOH and purged with argon for 30 min. Hydrogen sulphide (H_2S) was bubbled through the solution for 60 min. at the rate of 0.5 mL min^{-1}. 0.1 g of photocatalyst (PQ: TiO_2) was introduced in to the reactor and irradiated with the visible-light source (Xe-lamp Oriel, 450 W) at a constant stirring with continuous H_2S bubbling (0.5 mL/min). The excess H_2S was trapped in (0.5M) NaOH solution. The amount of evolved H_2 was measured using graduated gas burette and analyzed using Gas Chromatograph (Model Shimadzu GC-14B, MS-5 Å column, TCD, Ar carrier).

Acknowledgements

BBK would like to thank Department of Electronics and Information Technology (DeitY), Govt. of India for financial support and C-MET for providing research facilities. VUP gratefully acknowledges Council of Scientific and Industrial Research, CSIR, New Delhi, India for financial support.BBK and CJP would like to acknowledge the support by MSIP (Ministry of Science, ICT & future planning), Korea through Brain Pool program.

Notes and references

[a]*Centre for Materials for Electronics Technology (C-MET), Department of Electronics and Information Technology (DeitY), Govt. of India. Off Pashan Road, Panchwati, Pune-411008, India (kbbb1@yahoo.com)*
[b]*Department of Physics, University of Pune, Pune-411007, India*
[c]*Department of Materials Science and Engineering, Chonnam National University77, Yongbongro, Bukgu, Gwangju, South Korea.(parkcj@jnu.ac.kr)*

1 H. Kind, H. Yan, B. Messer, M. Law, P. D. Yang, *Adv. Mater.,* 2002, **14**, 158.
2 M. H. Huang, S. Mao, H. Feick, H. Yan, Y. Wu, H. Kind, E. Weber, R. Russo, P. D. Yang, *Science.,* 2001, **92**, 1897.
3 X. Fang, Y. Bando, M. Liao, U. K. Gautam, C. Zhai, B. Dierre, B. Liu, T. Sekiguchi, Y. Koide, D. Golberg, *Adv. Mater.,* 2009, **21**, 2034.
4 Z. B. He , J. S. Jie , W. J. Zhang , W. F. Zhang , L. B. Luo , X. Fan , G. D. Yuan , I. Bello, S. T. Lee, *Small.,* 2009, **5**, 345.
5 X. Chen, C. Li, M. Gratzel, R. Kosteckid, S. S. Mao, *Chem. Soc. Rev*., 2012, **41**, 7909.
6 M. Gratzel, *Nature.,* 2001, **414**, 338.
7 T. Y. Zhai, Z. J. Gu, H. Z. Zhong, Y. Dong, Y. Ma, H. B. Fu, Y. F. Li, J. N. Yao, *Cryst. Growth Des.,*2007, **7**, 488.
8 B. B. Kale, J. O. Baeg, S. M. Lee, H. Chang, S. J. Moon, C. W. Lee,*Adv. Funct. Mater.,* 2006,**16**, 1349.
9 P. Zhang, J. Zhang, J. Gong, *Chem. Soc. Rev*., 2014, **43**, 4395.
10 K. E. deKrafft, C. Wang, W. Lin, *Adv. Mater.,* 2012, **24**, 2014.
11 L. Liu, Z. Liu, A. Liu, X. Gu, C. Ge, F. Gao, L. Dong, *ChemSusChem.,* 2014, **7**, 618.
12 X. Zong, J. Han, B. Seger, H. Chen, G. Lu, C. Li, L. Wang, *Angew. Chem. Int. Ed*., 2014, **53**, 4399.
13 S. K. Apte, S. N. Garaje, G. P Mane, A. Vinu, S. D. Naik, D. P. Amalnerkar, B. B. Kale, *small.,* 2011, **7**, 957.
14 N. S. Chaudhari, A. P. Bhirud, R. S. Sonawane, L. K. Nikam, S. S. Warule, V. H. Rane, B. B. Kale,*Green Chem*., 2011, **13**, 2500.
15 N. S. Chaudhari, S. S. Warule, S. A. Dhanmane, M. V. Kulkarni, M. Valant, B. B. Kale, *Nanoscale*., 2013, **5**, 9383.
16 V. U. Pandit, S. S. Arbuj, U. P. Mulik, B. B. Kale, *Environ. Sci. Technol.,* 2014, **48**, 4178.
17 P. V. Kamat,*J. Phys. Chem. B.,* 2002,**106**, 7729.
18 A. Gasparotto, P. Fornasiero, G. V. Tendeloo, D. Barreca, V. Gombac, D. Bekermann, O. I. Lebedev, E. Tondello, A. Devi, C. Maccato, R. A. Fischer, T. Montini, *J. Am. Chem. Soc*., 2011, **133**, 19362.
19 D. Barreca, P. Fornasiero, A. Gasparotto, V. Gombac, C. Maccato, A. Pozza, E. Tondello, *Chem. Vap. Deposition,* 2010, **16**, 296.
20 M. Cargnello, A. Gasparotto, D. Barreca, V. Gombac, P. Fornasiero, T. Montini, *Eur. J. Inorg. Chem.,* 2011, **28**, 4309.
21 C. Maccato, D. Barreca, G. Carraro, A. Gasparotto, V. Gombac, P. Fornasiero, *Surface & Coatings Technology*, 2013, **230** , 219.
22 G. Carraro, C. Maccato, A. Gasparotto, T. Montini, S. Turner, O. I. Lebedev, V. Gombac, G. Adami, G. Tendeloo, D. Barreca, P. Fornasiero, *Adv. Funct.Mater.* 2014, **24**, 372.
23 D. Barreca, G. Carraro, V. Gombac, A. Gasparotto, C. Maccato, P. Fornasiero, E. Tondello, *Adv. Funct. Mater.* 2011, **21**, 2611.
24 N. Li, G. Liu, C. Zhen, F. Li, L. Zhang, H. M. Cheng, *Adv. Funct. Mater.,* 2011, **21**, 1717.
25 L. L. Tan, S. P. Chai, A. R. Mohamed, *ChemSusChem.,* 2012, **5**, 1868.
26 G. Xie, K. Zhang, B. Guo, Q. Liu, L. Fang, J. R. Gong, *Adv. Mater.,* 2013, **25**, 3820.
27 J. S. Lee, K. H. You, C. B. Park, *Adv. Mater.,* 2012, **24**, 1084.
28 W. Qian, P. A. Greaney, S. Fowler, S. K. Chiu, A. M. Goforth, J. Jiao, *ACS Sustainable Chem. Eng*., 2014, **2**, 1802.
29 T. Hirakawa, P. V. Kamat, *J. Am. Chem. Soc*., **2005**, **127**, 3928.
30 R. Liu, P. Wang, X. Wang, H. Yu, J. Yu, *J. Phys. Chem. C*, 2012, **116**, 17721.
31 C. T. Dinh, H. Yen, F. Kleitz, T.O. Do, *Angew. Chem. Int. Ed*., 2014, **53**, 6618.
32 Z. Bian, T. Tachikawa, P. Zhang, M. Fujitsuka, T. Majima, *J. Am. Chem. Soc*., 2014, **136**, 458.
33 T. Kamegawa, S. Matsuura, H. Seto, H. Yamashita, *Angew. Chem. Int. Ed*., 2013, **52**, 916.
34 B. Seger, P. V. Kamat, *J. Phys. Chem. C,* 2009, **113**, 18946.
35 C. Lin, Y. Song, L. Cao, S. Chen, *Nanoscale.*, 2013, **5**, 4986.
36 S. Pradhan, D. Ghosh, S. W. Chen, *ACS Appl. Mater. Interfaces*., 2009, **1**, 2060.
37 M. M. Khan, S. A. Ansari, D. Pradhan, M. O. Ansari, D. H. Han, J. Lee, M. H. Cho, *J. Mater. Chem. A*, 2014, **2**, 637.
38 J. Y. Kim, D. Lee, H. J. Kim, I. Lim, W. I. Lee, D. J. Jang, *J. Mater. Chem. A*, 2013, **1**, 5982.
39 R. Zhu, C. Y. Jiang, B. Liu, S. Ramakrishna, *Adv. Mater*., 2009, **21**, 994.
40 W. Ho, J.Yu, J. Lin, J. Yu, P. Li, *Langmuir*, 2004, **20**, 5865.